

**Planar magnetic interactions in the hulsite-type oxyborate  $\text{Co}_{5.52}\text{Sb}_{0.48}(\text{O}_2\text{BO}_3)_2$** 

D. C. Freitas, R. B. Guimarães, and J. C. Fernandes

*Instituto de Física, Universidade Federal Fluminense, Campus da Praia Vermelha, 24210-346 Niterói, RJ, Brazil*

M. A. Continentino

*Centro Brasileiro de Pesquisas Físicas, Rua Dr. Xavier Sigaud, 150 Urca, 22290-180 Rio de Janeiro, RJ, Brazil*

C. B. Pinheiro

*Departamento de Física, Instituto de Ciências Exatas, Universidade Federal de Minas Gerais, Campus da Pampulha, Caixa Postal 702, 30123-970 Belo Horizonte, MG, Brazil*

J. A. L. C. Resende

*Instituto de Química, Universidade Federal Fluminense, Campus do Valonguinho, 24020-141 Niterói, RJ, Brazil*

G. G. Eslava and L. Ghivelder

*Instituto de Física, Universidade Federal do Rio de Janeiro, Caixa Postal 68528, 21945-970 Rio de Janeiro, RJ, Brazil*

(Received 9 February 2010; revised manuscript received 15 April 2010; published 6 May 2010)

A large number of oxyborates studied up to now exhibit warwickite- or ludwigite-type structure with one-dimensional subunits (ladders or ribbons). The crystalline anisotropy strongly affects the physical properties of these systems. In this paper we present an extensive structural, magnetic, and thermodynamic study of an oxyborate  $\text{Co}_{5.52}\text{Sb}_{0.48}(\text{O}_2\text{BO}_3)_2$  with a hulsite-type structure. Differently from previously studied oxyborates, this material is characterized by the existence of planes in its structure which confers on it a strong two-dimensional (2D) character. This is manifested in the magnetic properties as shown by the low-temperature specific-heat results which are dominated by the contribution of two-dimensional antiferromagnetic magnons propagating in the planes. The 2D oxyborates opens the possibility of finding new and exciting behavior in these materials.

DOI: [10.1103/PhysRevB.81.174403](https://doi.org/10.1103/PhysRevB.81.174403)

PACS number(s): 75.50.-y, 75.30.Ds, 73.50.Fq, 75.40.-s

**I. INTRODUCTION**

The anhydrous oxyborates in which boron has trigonal coordination show, in general, highly anisotropic magnetic interactions. This is the case of those adopting the warwickite-,<sup>1</sup> ludwigite-,<sup>2,3</sup> and pyroborate-type<sup>4</sup> structures in which the anisotropy has a strong unidimensional character. An oxyborate adopting the hulsite-type structure, on the contrary, should present preferably quasiplanar magnetic interactions since the metal sites in this structure form two families of parallel sheets.<sup>5,6</sup> Our aim in studying a cobalt-antimony hulsite-type oxyborate was to observe the magnetic behavior of the metal ions in such a structure and to compare it to those of the already studied cobalt ludwigite-type compounds. For that we have synthesized a cobalt-based hulsite and carried-out measurements of its magnetization, dc and ac magnetic susceptibilities and specific heat under applied magnetic fields up to 9 T. All these measurements were performed down to 2 K. A single-crystal x-ray diffraction study of this material at room temperature and at 120 K is also included. This study not only checks the quality of our crystals but gives important structural information.

In the anhydrous oxyborates the metal ions are located within oxygen octahedra. This is the case of the hulsite in which there are five different crystallographic metal sites. All of them have multiplicity one except the M5 site which appears twice in the unit cell. In the planes formed by the sites M1 and M4 the octahedra share six edges so that the metal sites form a hexagonal lattice. In those planes containing the

sites M2 and M3 the octahedra share only four edges and this arrangement generates a rectangular metal lattice. These two sheets alternate along the crystal structure. They are held together by corner-linking to boron-oxygen triangles and to the oxygen octahedra around the metal sites M5. See Figs. 1 and 2.

The known natural hulsites have iron-based chemical compositions.<sup>5,6</sup> To our knowledge there is only one synthesized hulsite-type compound other than that studied in the present work. This is the  $\text{Ni}_{5.33}\text{Sb}_{0.67}(\text{O}_2\text{BO}_3)_2$  obtained by Bluhm *et al.*<sup>7</sup> in which nickel appears exclusively as  $\text{Ni}^{2+}$  ions. A cobalt based hulsite, on the contrary, could have divalent and trivalent ions and so to be a semiconductor. We looked then for a cobalt oxyborate adopting the hulsite-type structure and having the smallest possible content of  $\text{Sb}^{5+}$  ions so that the largest possible concentration of  $\text{Co}^{3+}$  ions should be obtained. The compound we found is  $\text{Co}_{5.52}\text{Sb}_{0.48}(\text{O}_2\text{BO}_3)_2$ . We remark however that the number of  $\text{Co}^{3+}$  ions present in this chemical composition is not sufficient to completely fill one of the six metal sites in the crystal.

This new hulsite-type oxyborate, in which the M2-M3 planes are exclusively occupied by cobalt ions, becomes rather interesting if we compare its properties to those of the cobalt oxyborates recently studied. These are the homometallic<sup>8</sup>  $\text{Co}_3\text{O}_2\text{BO}_3$  and the heterometallic<sup>9</sup>  $\text{Co}_5\text{Ti}(\text{O}_2\text{BO}_3)_2$  ludwigite-type compounds. The cobalt hulsite has obviously a different crystallographic structure but an intermediate amount of diluted nonmagnetic ions (Sb).

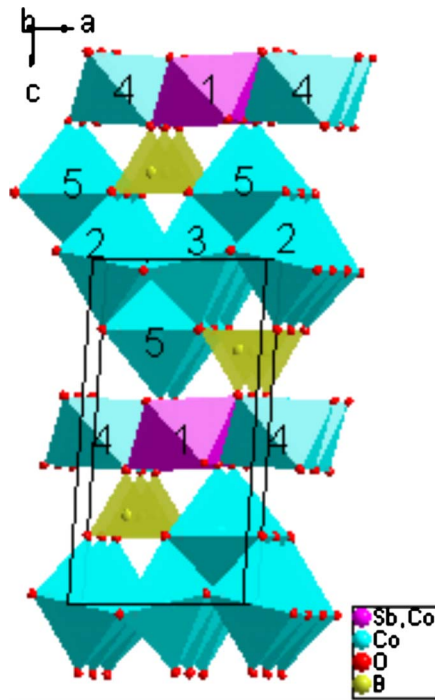


FIG. 1. (Color online) The schematic 3D structure of the hulsite. The oxygen polyhedra centered on the metal ions are shown. The numbers indicate metal sites and the lines indicate the  $a$  and  $c$  axes of the unit cell. The boron ions have trigonal coordination. This figure was generated by DIAMOND 2.1E software (Ref. 15).

We observe that the magnetic properties of the cobalt hulsite are not very different from those of the homometallic cobalt ludwigite since both present magnetic order below 42 K. The heterometallic ludwigite  $\text{Co}_5\text{Ti}(\text{O}_2\text{BO}_3)_2$ , we remark, presents a spin-glass configuration below 19 K. The specific heat of the hulsite, however, is as large as that of the heterometallic ludwigite. At low temperatures, as we show below, it presents a  $T^2$  temperature dependence with a small gap under a strong applied field. This behavior is unique among the already studied oxyborates and it indicates the existence of two-dimensional magnons, most probably propagating in the M2-M3 planes. This paper reports the synthesis method and the results of our structural, magnetic, and thermodynamic measurements for the hulsite  $\text{Co}_{5.52}\text{Sb}_{0.48}(\text{O}_2\text{BO}_3)_2$ .

## II. SYNTHESIS OF THE SAMPLE

The crystals were synthesized from a 26.5:2.5:8 molar mixture of  $\text{CoO}:\text{Sb}_2\text{O}_5:\text{HBO}_3$ . The mixture was fired in borax at 1150 °C for 24 h and slowly cooled down to 600 °C. The bath was dissolved in hot water and the crystals washed in diluted cold hydrochloric acid. Needle-shaped black crystals up to 0.3-mm long were obtained. The crystals chosen for measurements were those which presented the most brilliant and smooth faces as seen under a microscope.

## III. X-RAY DIFFRACTION

A prism-shaped single crystal was employed for data collection from x-ray diffraction. The measurements were car-

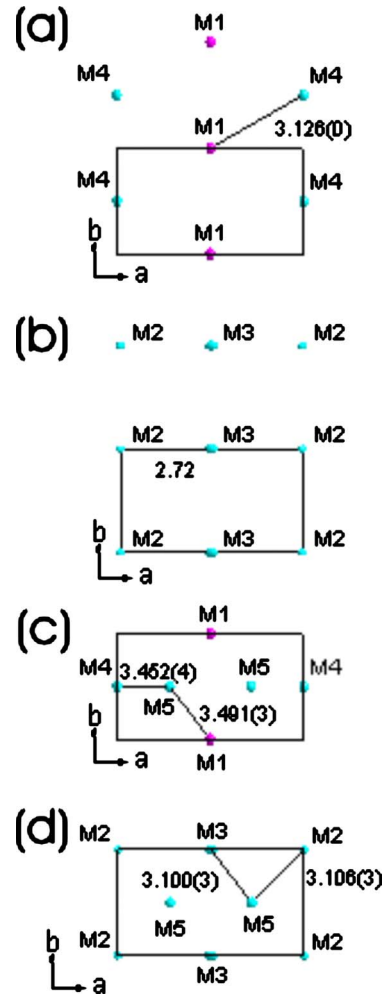


FIG. 2. (Color online) The metal sites in the  $ab$  planes of the hulsite  $\text{Co}_{5.52}\text{Sb}_{0.48}(\text{O}_2\text{BO}_3)_2$  at: (a)  $z/c=0.5$  and (b)  $z/c=0$ . In panels (c) and (d) the same planes appear with the projections of the nearest M5 sites. The distances are given in angstrom and the sides  $a$  and  $b$  of the unit cell are shown in each panel and given in Table I. These panels were generated by DIAMOND 2.1E software (Ref. 15).

ried out on an Xcalibur Atlas Gemini ultradiffractometer with graphite monochromated  $\text{Mo } K\alpha$  radiation ( $\lambda=0.71073$  Å). Low-temperature measurements were made using an Oxford Cryosystem device. The data collection, cell refinements, and data reduction were performed using the CRYSLISPRO software.<sup>10</sup> Data were collected up to  $69.6^\circ$  in  $2\theta$ . Analytical numeric absorption correction using a multifaceted crystal model was applied.<sup>11</sup> The structure was solved using the software SHELXS-97 (Ref. 12) and refined using the software SHELXL-97.<sup>13</sup> All atoms were clearly solved and full-matrix least-squares refinement procedures on  $F^2$  with anisotropic thermal parameters was carried on using SHELXL-97. Tables were generated by WINGX.<sup>14</sup> Crystal data, data-collection parameters, and structure-refinement data are summarized in Table I.

We resolved the structure at 290 and 120 K, in analogous experimental conditions, in order to observe any eventual conformational change with temperature. No evidence for any phase transition was found. Figure 1 shows a schematic three-dimensional (3D) structure of the hulsite and the oxy-

TABLE I. Crystal data and structure refinement of the cobalt antimonium hulsite sample.

Chemical composition from x-ray analysis	$\text{Co}_{5.52}\text{Sb}_{0.48}(\text{O}_2\text{BO}_3)_2$	
Formula weight	565.35	
Wavelength	0.717073 Å	
Crystal size	0.1054 × 0.0440 × 0.0382 mm <sup>3</sup>	
Temperature	290(2) K	120(2) K
Crystal system	Monoclinic	Monoclinic
Space group	$P12/m1$ ( $n^\circ.10$ )	$P12/m1$ ( $n^\circ.10$ )
Unit-cell dimension $a=$	5.4395(2) Å	5.43460(10) Å
$b=$	3.08050(10) Å	3.07710(10) Å
$c=$	10.6335(3) Å	10.6307(2) Å
$\beta=$	94.092(3)°	94.122(2)°
Volume	177.725(10) Å <sup>3</sup>	177.315(7) Å <sup>3</sup>
$Z$	1	1
Density (calculated)	5.282 Mg/m <sup>3</sup>	5.294 Mg/m <sup>3</sup>
Absorption coefficient	14.433/mm	14.466/mm
$F(000)$	264	264
$\theta$ range (degrees)	3.76–30.47	3.76–34.87
Index range $h=$	–7, 7	–8, 8
$k=$	–4, 4	–4, 4
$l=$	–15, 15	–16, 16
Reflections collected	3691	8523
Independent reflections	634	865
$R(\text{int})$	0.0346	0.0366
Completeness	99.8% to $\theta=30.47$	98.2% to $\theta=34.87$
Absorption correction	Analytical	Analytical
Max./min. transmission	0.6086/0.3115	0.6080/0.3109
Refinement method: full-matrix least squares on $F^2$		
Data/restraints/parameters	634/0/61	865/0/61
Goodness-of-fit on $F^2$	1.079	1.067
Final $R$ indices [ $I > 2\sigma(I)$ ]	$R1=0.0201$	$R1=0.0183$
	$wR2=0.0499$	$wR2=0.0433$
$R$ indices (all data)	$R1=0.0235$	$R1=0.0228$
	$wR2=0.0509$	$wR2=0.0444$
Extinction coefficient	0.0080(19)	0.0063(13)
Largest diff. peak	1.429 e Å <sup>–3</sup>	1.817 e Å <sup>–3</sup>
Largest diff. hole	–0.797 e Å <sup>–3</sup>	–1.001 e Å <sup>–3</sup>

gen polyhedra around the metal ions. Sites 1 are occupied by Sb and Co ions in a disordered way and no other metal site contains Sb ions. Panels in Fig. 2 show the planes formed by the metal sites. The refinement of the metal sites occupancies yield to the chemical formula  $\text{Co}_{5.52}\text{Sb}_{0.48}(\text{O}_2\text{BO}_3)_2$  for our sample in agreement with the electronic microscopy measurements. The bond lengths and the bond angles are given in Tables II and III, respectively. The averages of the B-O bond lengths and of the O-B-O bond angles are in good agreement with the expected trigonal planar geometry. Table IV shows the fractional coordinates and the sites occupation factors.

#### IV. MICROSCOPY ANALYSIS

Electron probe wavelength dispersive x-ray spectroscopy (WDS) measurements were performed in a JEOL JCXA-8900RL equipment. Selected crystals were mounted on a sample holder using carbon conductive tape. The following working conditions were used: acceleration voltage 15 kV, beam current 20 nA collimated into a sample dot approximately 1- $\mu$  diameter. The analytical x-ray lines used were Co  $K\alpha$  and Sb  $L\alpha$ .

The average chemical composition found for several different crystals is  $\text{Co}_{5.48}\text{Sb}_{0.52}(\text{O}_2\text{BO}_3)_2$ . This formula is com-

TABLE II. Selected M-O and B-O bond lengths in Å for  $\text{Co}_{5.52}\text{Sb}_{0.48}(\text{O}_2\text{BO}_3)_2$ . The underline numbers are the symmetry codes: (i)  $x-1, y, z$ ; (ii)  $x, y+1, z$ ; (iii)  $x, y-1, z$ ; (iv)  $x+1, y, z$ ; (v)  $-x+1, -y, -z+1$ ; (vi)  $-x+1, -y, -z+2$ ; (vii)  $-x, -y-1, -z+1$ ; (viii)  $-x+1, -y-1, -z+1$ ; and (ix)  $-x, -y, -z+2$ . The intermetal distances are found in Fig. 2.

M1-O2	2.089(3)	M4-O4 <sub>i</sub>	2.051(3)
M1-O4	2.0369(18)	M5-O1	2.1690(19)
M2-O3	2.118(3)	M5-O3 <sub>iv</sub>	2.1695(19)
M2-O5 <sub>i</sub>	2.0777(18)	M5-O4	2.008(3)
M3-O1	2.109(3)	M5-O5	2.015(3)
M3-O5	2.0782(17)	B-O1	1.364(5)
M3-O5 <sub>ii</sub>	2.0782(18)	B-O2	1.410(5)
M4-O2	2.152(2)	B-O3	1.369(5)
M4-O2 <sub>iii</sub>	2.1523(19)		

patible with that found through x-ray analysis. In Fig. 3 we may see a backscattered electron image of some crystals.

## V. MAGNETIC MEASUREMENTS

Measurements of the magnetic properties of the hulsite  $\text{Co}_{5.52}\text{Sb}_{0.48}(\text{O}_2\text{BO}_3)_2$  have been carried out employing a commercial PPMS *platform Quantum Design*. The sample was an ensemble of randomly oriented crystals weighting 36.08 mg. The results of magnetic measurements are shown in the Figs. 4–7.

Figure 4 shows the inverse of magnetization curve versus temperature. The function  $1/M = 18.44 + 0.2688 \times T$  fits this curve in the paramagnetic region. From this fitting we obtain the Curie-Weiss temperature  $\theta = -69.9$  K and the average total angular momentum per cobalt ion  $\bar{J} = 2.31$ . This value means that the orbital angular moment is partially unquenched since it should be equal to 1.55 if both ions,  $\text{Co}^{2+}$  and  $\text{Co}^{3+}$ , were in the high spin state and their angular momentum completely quenched.

TABLE III. The largest O-M-O and the O-B-O bond angles in degrees for  $\text{Co}_{5.52}\text{Sb}_{0.48}(\text{O}_2\text{BO}_3)_2$ . The underline numbers are the symmetry codes (see Table II caption).

O2 <sub>v</sub> -M1-O2	180.0
O4 <sub>v</sub> -M1-O4	180.0
O3-M2-O3 <sub>ix</sub>	180.000(1)
O5 <sub>vi</sub> -M2-O5 <sub>i</sub>	180.0
O1 <sub>vi</sub> -M3-O1	180.0
O5-M3-O5 <sub>vi</sub>	180.000(1)
O2-M4-O2 <sub>vii</sub>	180.0
O4 <sub>viii</sub> -M4-O4 <sub>i</sub>	180.0
O4-M5-O5	178.47(11)
O1 <sub>iii</sub> -M5-O3 <sub>iv</sub>	168.49(11)
O1-B-O3	124.2(4)
O1-B-O2	118.5(3)
O3-B-O2	117.3(3)



FIG. 3. Photo of cobalt-antimonium hulsite-type crystals using backscattered electron imaging in WDS measurements.

Figure 5 exhibits the magnetization curves as a function of temperature for applied fields of 0.02 and 1 T (inset) in both regimens: field cooled and zero field cooled (zfc). Near 42 K the low field curves separate and the zfc curve shows an abrupt change in derivative. The Fig. 6 shows the ac susceptibilities. It must be remarked that the  $\chi'$  peak at 42 K does not move with frequency. The above results and the peak which appears in the specific-heat curve at this same temperature (see below) indicate that below 42 K there is an ordered magnetic phase where the interions couplings are mainly antiferromagnetic since the Curie-Weiss temperature is negative. Figure 7 shows the magnetization curves as a function of applied fields for different temperatures. Notice that below 20 K all these curves yield a magnetic moment of  $0.4\mu_B$  per formula unit at 9 T. This means that the average contribution per magnetic ion at these conditions is  $0.072\mu_B$ .

## VI. SPECIFIC-HEAT MEASUREMENTS

Specific-heat measurements as a function of temperature under applied magnetic fields of different intensities were performed employing 4.39 mg of crystals. The same PPMS *platform Quantum Design* equipment was used.

The panel *a* of the Fig. 8 shows the specific-heat curves plotted as  $C/T$  versus  $T$  for different cobalt oxyborates: the hulsite  $\text{Co}_{5.52}\text{Sb}_{0.48}(\text{O}_2\text{BO}_3)_2$  and the ludwigites  $\text{Co}_3\text{O}_2\text{BO}_3$  and  $\text{Co}_5\text{Ti}(\text{O}_2\text{BO}_3)_2$ . We may notice that the specific-heat values of the hulsite are much larger than those of the homometallic ludwigite and that both curves present a peak near 42 K indicating magnetic ordering below this temperature. This ordering is also suggested by the magnetic measurements which present features at this same temperature. In the panel *b* of the same figure the specific-heat curve of the hulsite, also plotted as  $C/T$  versus  $T$ , appear for different applied fields. We notice that the peak at 42 K smooths down but does not shift as the applied field increases. This indicates a type of magnetic order more complex than that of a conventional antiferromagnet. The fitting of the specific-heat curve shows clearly a  $T^2$  behavior in the low-temperature range with a small gap of 0.75 K for an applied magnetic field of 9 T (see Fig. 9). This is a clear indication of two-

TABLE IV. Fractional coordinates, site occupation factors (SOF) and the equivalent isotropic displacement parameters ( $\text{\AA}^2 \times 10^3$ ) for  $\text{Co}_{5.52}\text{Sb}_{0.48}(\text{O}_2\text{BO}_3)_2$ .  $U(\text{eq})$  is defined as one third of the trace of the orthogonalized  $U_{ij}$  tensor. The SOF values must be multiplied by the factor 4 in order to obtain the number of atoms in the unit cell (Ref. 16).

Site	$x/a$	$y/b$	$z/c$	SOF	$U(\text{eq})$
Co1	1/2	0	1/2	0.13	9(1)
Co2	0	0	1	1/4	5(1)
Co3	1/2	0	1	1/4	8(1)
Co4	0	-1/2	1/2	1/4	9(1)
Co5	0.718210	-1/2	0.780730	1/2	8(1)
Sb1	1/2	0	1/2	0.12	3(1)
O1	0.443397	0	0.801737	1/2	10(1)
O2	0.193968	0	0.608032	1/2	9(1)
O3	-0.000835	0	0.800747	1/2	10(1)
O4	0.680676	-1/2	0.591530	1/2	10(1)
O5	0.745994	-1/2	0.970733	1/2	13(1)
B	0.213893	0	0.741004	1/2	7(1)

dimensional magnons with a residual moment of  $0.124\mu_B$  at this field. If the order was that of an ordinary conventional antiferromagnet, the magnetic moments associated to each sublattice would obviously be one half of this value, i.e.,  $0.062\mu_B$  per ion. This value is not very far from that of  $0.072\mu_B$  found above for the magnetization at low temperatures under a field of 9 T.

From the above results we can evaluate the magnon speed and consequently the average exchange integral value. The energy per mol in the M2-M3 plane is given by the integral

$$E = \frac{AN}{(2\pi)^2} \int_0^\infty dk \frac{2\pi k c k}{\exp(\beta c k) - 1}, \quad (1)$$

where  $A$  is the inverse of the cobalt ions density in the M2-M3 plane obtained from Fig. 2(b),  $N$  is the number of cobalt ions per mol of the compound, and  $\beta$  has the usual meaning. The energy of the  $k$  state is assumed to be  $\epsilon_k = ck$  where  $c = \hbar v$  and  $v$  is the magnon speed. Setting  $x = \beta ck$  we get

$$E = \frac{AN}{(2\pi)^2} \frac{1}{c^2 \beta^3} \int_0^\infty \frac{x^2 dx}{\exp(x) - 1} \propto T^3. \quad (2)$$

The molar specific heat is given by

$$c_v = \frac{\partial E}{\partial T} = \frac{3AN}{2\pi} 2.4 \frac{k_B^3}{c^2} T^2 = a T^2. \quad (3)$$

The  $a$  value appears in Fig. 9. These results lead to

$$v^2 = \frac{7.2AN}{2\pi a \hbar^2} k_B^3. \quad (4)$$

Putting values we obtain  $v = 1.18 \times 10^3$  m/s without applied field and  $v = 1.30 \times 10^3$  m/s for  $H = 9$  T. If the magnon spectrum has a gap  $b$ , due to anisotropy or an external magnetic field, the specific heat has an extra exponential dependence required for the thermal activation of these excitations above the gap (see Fig. 9).

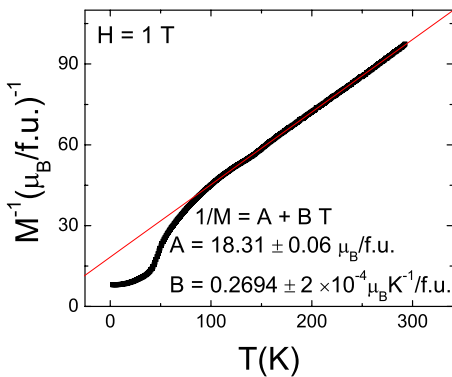


FIG. 4. (Color online) Inverse of magnetization versus temperature for the ludwigite-type oxyborate  $\text{Co}_{5.52}\text{Sb}_{0.48}(\text{O}_2\text{BO}_3)_2$ . The parameters of linear adjust for paramagnetic region are shown.

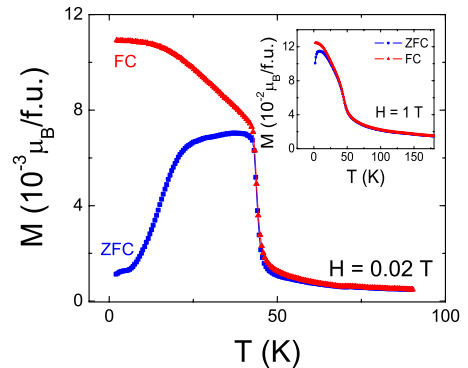


FIG. 5. (Color online) Magnetization versus temperature of the oxyborate  $\text{Co}_{5.52}\text{Sb}_{0.48}(\text{O}_2\text{BO}_3)_2$  under an applied field of 0.02 T for field-cooled and zero-field-cooled regimens. The inset shows the magnetization curves for an applied field of 1 T.



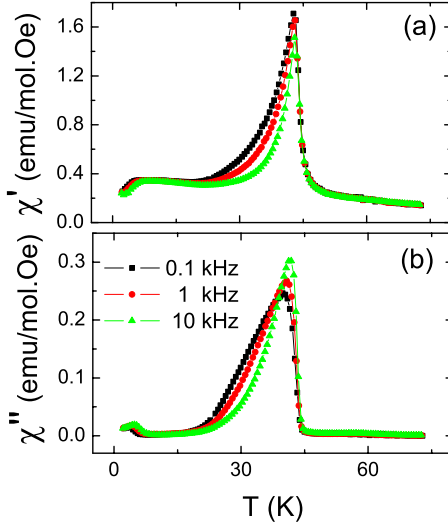


FIG. 6. (Color online) (a) Real parts of ac susceptibility versus temperature of the oxyborate  $\text{Co}_{5.52}\text{Sb}_{0.48}(\text{O}_2\text{BO}_3)_2$  at 0.1, 1, and 10 kHz. (b) Imaginary parts of the same susceptibility at the same frequencies. Both curves were measured under an applied field of 10 Oe.

Alternatively, from the spin-wave stiffness in zero magnetic field, we can obtain an average exchange interaction in the M2-M3 planes shown in Fig. 2. For a planar antiferromagnet with a linear dispersion relation for magnons,  $\epsilon_k = ck$ , the spin-wave stiffness is given by  $c = 8JSd/\sqrt{2}$ , where  $d$  is the average distance between metal ions. Using the results above and  $d = 2.9 \times 10^{-10}$  m for the M2-M3 planes we obtain an exchange constant (modulus)  $J = 0.31 \times 10^{-3}$  eV, where we used  $S = 3/2$ . On the other hand we can calculate  $J$  from the Curie-Weiss constant obtained from the data plotted in Fig. 4. Since  $\theta = S(S+1)zJ/3k_B$ , where  $z = 4$  is the number of nearest neighbors, we get  $J = 1.21 \times 10^{-3}$  eV using  $|\theta| = 69.9$ . Both values of  $J$  are of the correct order of magnitude and consistent with the value of the ordering temperature  $T_N = 42$  K. Also the paramagnetic Curie temperature obtained at high temperatures gives an average over the magnetic couplings in the whole three-dimensional lattice, some of which may be frustrated in the disordered hexagonal planes. It is reasonable then that the average exchange cou-

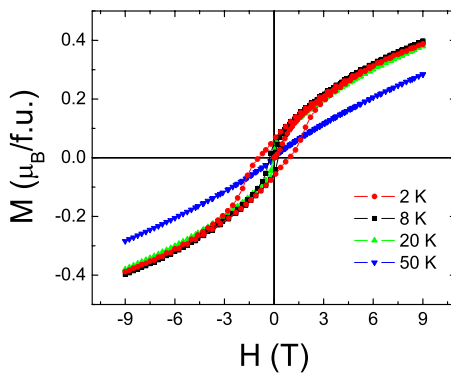


FIG. 7. (Color online) Magnetization of the oxyborate  $\text{Co}_{5.52}\text{Sb}_{0.48}(\text{O}_2\text{BO}_3)_2$  versus applied magnetic field for different temperatures.

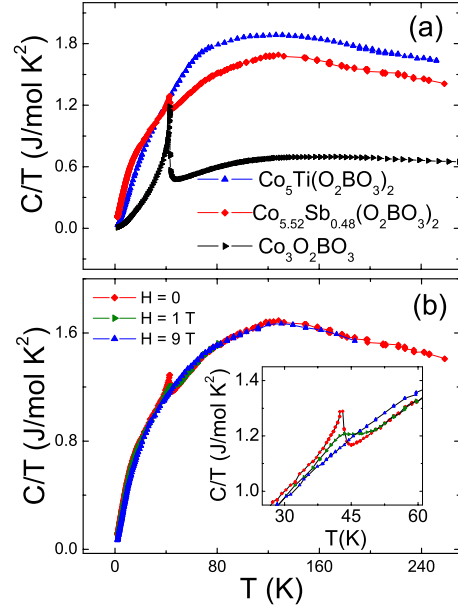


FIG. 8. (Color online) (a) Specific-heat curve plotted as  $C/T$  versus  $T$  for  $\text{Co}_{5.52}\text{Sb}_{0.48}(\text{O}_2\text{BO}_3)_2$  (present work). The curves for the ludwigite-type oxyborates  $\text{Co}_3\text{O}_2\text{BO}_3$  and  $\text{Co}_5\text{Ti}(\text{O}_2\text{BO}_3)_2$  are taken from Refs. 8 and 9, respectively. (b) Specific-heat curves under three different applied fields for the oxyborate  $\text{Co}_{5.52}\text{Sb}_{0.48}(\text{O}_2\text{BO}_3)_2$ . The inset shows a zoom in the peak near 42 K.

pling obtained from the paramagnetic  $\theta$  turns out to be larger than that associated with the low-temperature excitations.

### VII. DISCUSSION

The physics of low-dimensional magnetic materials is an exciting area of research in condensed matter. The strong fluctuations in these reduced dimensionalities give rise to new effects and many unexpected results. The study of the oxyborates with warwickite and ludwigite-type structures which contain one-dimensional subunits in the form of ribbons and ladders have fulfilled these expectations exhibiting a rich variety of behavior.<sup>17</sup> The present investigation of the

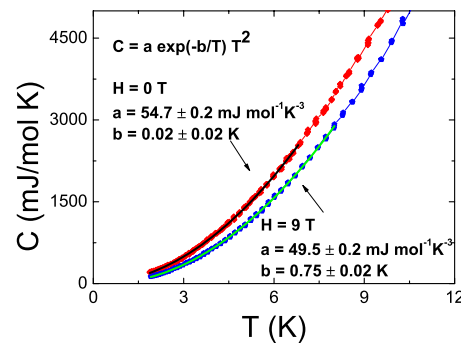


FIG. 9. (Color online) Low-temperature range of the specific-heat curves of the hulsite-type oxyborate  $\text{Co}_{5.52}\text{Sb}_{0.48}(\text{O}_2\text{BO}_3)_2$  under different applied fields. Fitting by the function  $C = a \exp(-b/T) T^2$  is also shown.

oxyborate  $\text{Co}_{5.52}\text{Sb}_{0.48}(\text{O}_2\text{BO}_3)_2$  system, with a hulsite-type structure, adds a dimension on the study of these materials. The existence of planes where the transition metals are located is clearly revealed and characterized in the present study. These planes are magnetically ordered at low temperatures. The order is of the antiferromagnetic type as shown by the value of the ordered moments and is consistent with the predominant antiferromagnetic interactions implied by the high-temperature Curie constant. The specific-heat result at low temperatures is dominated by a  $T^2$  contribution. As we have shown this term is due to magnons with a linear dispersion relation propagating in planes and gives unambiguous evidence of the two-dimensional nature of the magnetic ordering. The spectrum of magnon excitations has a small gap

which guarantees the possibility of magnetic long-range order. Otherwise this would be unstable in two dimensions. This gap is related to the partial unquenching of the magnetic moment which has an orbital contribution as shown by the value of the magnetic moments extracted from the magnetic data. The possibility of studying two-dimensional phenomena in magnetic oxyborates opens new perspectives which are surely worth continuing to explore.

#### ACKNOWLEDGMENTS

Support from the Brazilian agencies CNPq and FAPERJ is gratefully acknowledged.

\*mucio@if.uff.br

<sup>1</sup>J. C. Fernandes, R. B. Guimarães, M. A. Continentino, H. A. Borges, J. V. Valarelli, and A. Lacerda, *Phys. Rev. B* **50**, 16754 (1994).

<sup>2</sup>M. Mir, J. C. Fernandes, M. A. Continentino, A. C. Doriguetto, Y. P. Mascarenhas, J. Ellena, E. E. Castellano, R. S. Freitas, and L. Ghivelder, *Phys. Rev. Lett.* **87**, 147201 (2001).

<sup>3</sup>P. Bordet and E. Suard, *Phys. Rev. B* **79**, 144408 (2009).

<sup>4</sup>J. C. Fernandes, R. B. Guimarães, M. A. Continentino, R. Rapp, Y. Blancquaert, S. Yates, and C. Paulsen, *Phys. Rev. B* **69**, 054418 (2004).

<sup>5</sup>N. A. Yamnova, M. A. Simonov, and N. V. Belov, *Kristallografiya* **20**, 156 (1975).

<sup>6</sup>J. A. Konnert, D. E. Appleman, J. R. Clark, L. W. Finger, T. Kato, and Y. Miura, *Am. Mineral.* **61**, 116 (1976).

<sup>7</sup>K. Bluhm, H. K. Müller-Buschbaum, and L. Walz, *J. Less-Common Met.* **158**, 339 (1990).

<sup>8</sup>D. C. Freitas, M. A. Continentino, R. B. Guimarães, J. C. Fernandes, J. Ellena, and L. Ghivelder, *Phys. Rev. B* **77**, 184422 (2008).

<sup>9</sup>D. C. Freitas, R. B. Guimarães, D. R. Sanchez, J. C. Fernandes, M. A. Continentino, J. Ellena, A. Kitada, H. Kageyama, G. G. Eslava, and L. Ghivelder, *Phys. Rev. B* **81**, 024432 (2010).

<sup>10</sup>CRYALISPRO, Oxford Diffraction Ltd., Version 1.171.33.41 (release 06-05-2009 CrysAlis 171.NET).

<sup>11</sup>R. C. Clark and J. S. Reid, *Acta Crystallogr., Sect. A: Found. Crystallogr.* **51**, 887 (1995).

<sup>12</sup>SHELXS97—Program for Crystal Structure Solution (Release 97-2). G. M. Sheldrick, Institut für Anorganische Chemie der Universität, Tammanstrasse 4, D-3400 Göttingen, Germany, 1998.

<sup>13</sup>SHELXL97—Program for Crystal Structure Refinement (Release 97-2). G. M. Sheldrick, Institut für Anorganische Chemie der Universität, Tammanstrasse 4, D-3400 Göttingen, Germany, 1998.

<sup>14</sup>L. J. Farrugia, *J. Appl. Crystallogr.* **32**, 837 (1999).

<sup>15</sup>G. Bergerhoff, M. Berndt, and K. Brandenburg, *J. Res. Natl. Inst. Stand. Technol.* **101**, 221 (1996).

<sup>16</sup>International Tables for Crystallography 5th ed., edited by Theo Hahn (Springer, Dordrecht, The Netherlands, 2005), Vol. A, p. 161.

<sup>17</sup>See M. A. Continentino, J. C. Fernandes, R. B. Guimarães, B. Boechat, and A. Saguia, in *Magnetism in Highly Anisotropic Borates: Experiment and Theory*, Frontiers in Magnetic Materials, edited by A. V. Narlikar (Springer, New York, 2005), pp. 385-410.